

Magnetic Quantum Dot: A Magnetic Transmission Barrier and Resonator

H.-S. Sim,^{1,*} G. Ihm,² N. Kim,³ and K.J. Chang¹

¹*Department of Physics, Korea Advanced Institute of Science and Technology, Taejeon 305-701, Korea*

²*Department of Physics, Chungnam National University, Taejeon 305-764, Korea*

³*Quantum-Functional Semiconductor Research Center, Dongguk University, Seoul 100-715, Korea*

(Received 9 March 2001; published 14 September 2001)

We study the ballistic edge-channel transport in quantum wires with a magnetic quantum dot, which is formed by two different magnetic fields B^* and B_0 inside and outside the dot, respectively. We find that the electron states located near the dot and the scattering of edge channels by the dot strongly depend on whether B^* is parallel or antiparallel to B_0 . For parallel fields, two-terminal conductance as a function of channel energy is quantized except for resonances, while, for antiparallel fields, it is not quantized and all channels can be completely reflected in some energy ranges. All these features are attributed to the characteristic magnetic confinements caused by nonuniform fields.

DOI: 10.1103/PhysRevLett.87.146601

PACS numbers: 72.15.Gd, 73.20.-r, 73.23.Ad, 73.40.-c

Transport properties of two-dimensional electron gas (2DEG) in spatially nonuniform magnetic fields have attracted much attention. Various magnetic structures such as magnetic dots [1], superlattices [2], barriers [3], and transverse steps [4] were realized experimentally in nonplanar 2DEGs or by patterning ferromagnetic or superconducting materials. Theoretically, it was shown that nonuniform magnetic fields can cause electron drifts [5,6], transmission barriers [7], and commensurability effects [8]. Magnetic edge states, which exist along the boundary between two different magnetic domains, were proposed [9,10] in the analogy with the conventional edge states [11] in quantum Hall systems, and their effects on magnetoresistance were reported experimentally [4].

The electron transport through quantum wires in strong magnetic fields can be well described by edge channels. When a local electrostatic modulation is applied additionally inside the wires, conductances can be still quantized and resonant reflections appear [12,13]. These interesting features can be modified when such a modulation is replaced by a magnetic one such as a magnetic quantum dot (or magnetic antidot) [9,10], which is formed in 2DEG by nonuniform perpendicular magnetic fields; $\vec{B} = B^*\hat{z}$ within a circular disk with radius r_0 , while $\vec{B} = B_0\hat{z}$ outside it. The classical electron trajectories (see Fig. 1) scattered by a magnetic dot with $\gamma [= B^*/B_0] < 0$ are very different from those for $\gamma > 0$ and those by an electrostatic dot or antidot, indicating distinct edge-channel scatterings by local magnetic modulations from those by electrostatic ones. The study of such a scattering mechanism is important to understanding the electron transport in magnetic structures and to suggesting future device applications. However, to our knowledge, little attention has been paid to it [7].

In this Letter, we study the ballistic transport of conventional edge channels through quantum wires with a magnetic quantum dot. The magnetic edge states near the dot and the two-terminal conductance $G(E_F)$ of the wires in the zero bias limit are found to exhibit distinct features be-

tween two cases of $\gamma > 0$ and $\gamma < 0$, where E_F is the Fermi energy. For $\gamma > 0$, $G(E_F)$ is quantized and the dot behaves as a transmission barrier and a resonator, when the magnetic length inside the dot is smaller than r_0 . This feature results from the harmonic-potential-like magnetic confinements and is similar to that of electrostatic modulations. On the other hand, for $\gamma < 0$, $G(E_F)$ is not quantized when incident channels are scattered by the dot. Moreover, for $\gamma < -1$, all incident channels can be completely reflected by the dot in some ranges of E_F , resulting in the plateaus of $G(E_F) = 0$. These interesting features for $\gamma < 0$ are due to the double-well and merged-well magnetic confinements caused by the field reversal at the dot boundary. We also propose a calculational method for conductances, based on the symmetric gauge and Green's function.

The dot is located in the middle of an infinitely long wire, whose potential is an infinite square well of width L_y in the transverse y direction (see Fig. 1). The distance between the dot and wire edge is Δ . The magnetic length and the Landau energy inside (outside) the dot are determined by B^* (B_0) as $l_{B^*}(j) = \sqrt{(2j+1)\hbar/(e|B^*|)}$ [$l_{B_0}(j) = \sqrt{(2j+1)\hbar/(eB_0)}$] and $E^*(j) = (j+1/2)\hbar e|B^*|/m^*$ [$E_0(j) = (j+1/2)\hbar eB_0/m^*$], respectively, where $j = 0, 1, 2, \dots$ and m^* is the effective mass. We focus on the edge state transport regime, i.e., $L_y \gg l_{B_0}(N-1)$, and

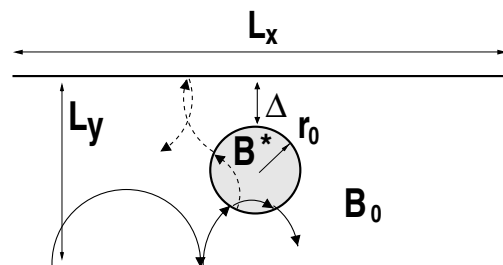


FIG. 1. Schematic diagram of a quantum wire with a magnetic quantum dot. Solid (dashed) arrows represent the classical electron trajectories for $B^*/B_0 > 0$ ($B^*/B_0 < 0$).

ignore the effects of spin and disorder, where N is the number of Landau levels below E_F far away from the dot.

We first consider the case for $\Delta > l_{B_0}(N - 1)$. In this case, incident conventional edge channels do not interact with the dot, thus, $G(E_F) = NG_0$ (including the spin degeneracy) except for backward scatterings of channels by the resonant tunneling into the magnetic edge states of the dot, where $G_0 = 2e^2/h$. To understand these magnetic edge states, we examine a magnetic dot in an infinite 2DEG. When the dot center is located at $r = 0$ in polar coordinates (r, θ) , the eigenstates can be written as $\psi_{nm}(\vec{r}) = R_{nm}(r)e^{im\theta}$ for the symmetric gauge, where m is the angular momentum quantum number and n ($= 0, 1, 2, \dots$) is the number of nodes in $R_{nm}(r)$.

The eigenstates can be classified by their radial locations. A $(n, m < 0)$ state located far away from the dot interacts with B_0 . From the gauge invariance [14], its radial wave function is found to be the same as that of the (n, m_{eff}) state in uniform fields B_0 . Here, $m_{\text{eff}} = m - s$ and s [$= (1 - \gamma)\pi r_0^2 B_0 / \phi_0$] is the number of removed magnetic flux quanta (or additional ones for $s < 0$) to form the magnetic dot in 2DEG where the uniform B_0 is already applied [9]. Then, $\psi_{nm < 0}$ is located at $r_p(m_{\text{eff}}, B_0)$ with the eigenenergy $E_{nm} = E_0(n)$, enclosing $|m|$ flux quanta, where $r_p(m, B) = \sqrt{2|m|\hbar/(eB)}$. On the other hand, ψ_{nm} 's near the dot interact with both B_0 and B^* , thus, E_{nm} 's deviate from $E_0(n)$. They are magnetic edge states circulating along the dot boundary [9] and cause resonant scatterings of conventional edge channels. When $r_0 \gg l_{B^*}(n - 1)$ and $|m|$ is small, ψ_{nm} 's are located at $r_p(m, B^*)$ inside the dot with $E_{nm} = E^*(n)$. Interestingly, for $\gamma < 0$, ψ_{nm} 's with small $m < 0$ can be located also at $r_p(m_{\text{eff}}, B_0)$ outside the dot.

The above features are clearly shown in Fig. 2. In dimensionless units of $E_0(0) \rightarrow 1$ and $\sqrt{2}l_{B_0}(0) \rightarrow 1$, we calculate E_{nm} 's from the radial part of the Schrödinger equation, $[d^2/dr^2 + d/(rdr) + 2(E_{nm} - V_{\text{eff}}(r))]R_{nm}(r) = 0$. Here, we define the *magnetic confinement* as the effective potential V_{eff} , where $V_{\text{eff}}(r) = (m/r + \gamma r)^2/2$ for $r < r_0$, while $V_{\text{eff}}(r) = (m_{\text{eff}}/r + r)^2/2$ for $r > r_0$. For $\gamma > 0$, $V_{\text{eff}}(r)$ is similar to the harmonic potential, which is the magnetic confinement in uniform fields. Thus, E_{nm} 's vary monotonously from $E_0(j)$ at large $|m|$ [i.e., $r_p(m_{\text{eff}}, B_0) \gg r_0$] to $E^*(j)$ at small $|m|$ [i.e., $r_p(m, B^*) \ll r_0$], where $j = n + (m + |m|)/2$. Note that for small r_0 [$< l_{B^*}(j)$], E_{nm} does not reach $E^*(j)$ at small $|m|$, as shown in Fig. 2(b). For $\gamma > 1$, magnetic edge states circulate counterclockwise around the dot, while either clockwise or counterclockwise for $0 < \gamma < 1$.

For $\gamma < 0$, magnetic confinements are very different from the harmonic potential. For $|m| < |\gamma|s_0$, V_{eff} is a double-well potential with a barrier at r_0 , where $s_0 = \pi r_0^2 B_0 / \phi_0$. The barrier is high enough to confine ψ_{nm} only in one of the wells, if $r_0 \gg l_{B^*}$. Then, for small $m < 0$, the inner well allows energies $E^*(j_1)$ with $j_1 = |m|$,

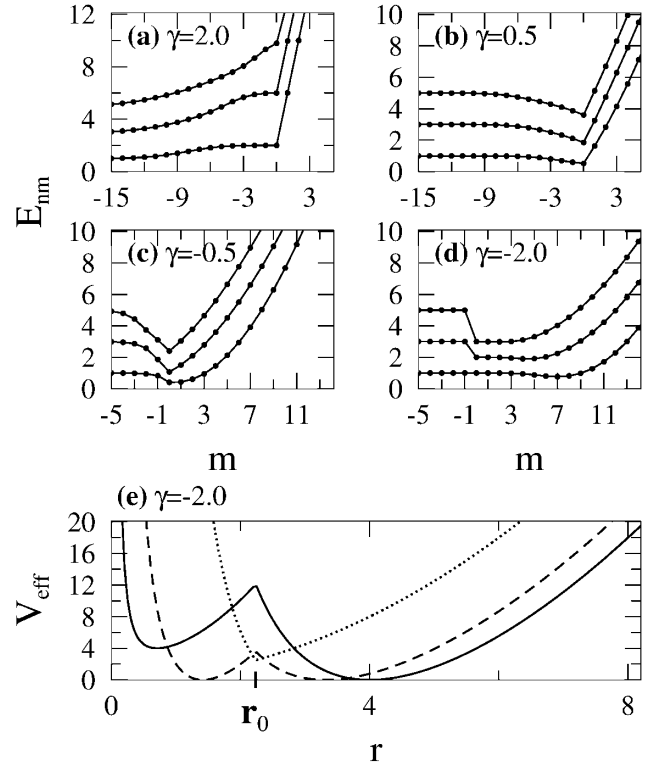


FIG. 2. (a)–(d) E_{nm} 's and (e) $V_{\text{eff}}(r, m)$'s for s_0 ($= \pi r_0^2 B_0 / \phi_0$) = 5 and some γ 's. In (e), $m = -1$ (solid), 4 (dashed), 15 (dotted) are chosen. The energy unit is $E_0(0)$.

$|m| + 1, |m| + 2, \dots$, while the outer well allows $E_0(j_2)$ with $j_2 = 0, 1, 2, \dots$. Thus, ψ_{nm} with small $m < 0$ can be located either inside or outside the dot, depending on n , as discussed before. This feature results in abrupt changes of E_{nm} 's from E_0 to E^* [see Fig. 2(d)]. Note that in Fig. 2(c) the abrupt change appears only in the $n = 0$ level, since $l_{B^*}(0) \approx r_0$. For $|\gamma|s_0 \leq m \leq s + s_0$, the two wells in V_{eff} merge into a single well with a minimum at r_0 [see the dotted line in Fig. 2(e)]. The magnetic edge states in this merged well circulate counterclockwise along $r = r_0$ with snakelike classical motions.

Next, we study the scattering of conventional edge channels by the magnetic dot when $\Delta \leq l_{B_0}(N - 1)$. We calculate the transmission probability $T(\alpha)$ [$= G(\alpha)/G_0$] of incident channels as a function of dimensionless energy α [$= E_F/(2E_0(0))$] using the lattice Green's function [13], where a continuous 2DEG is approximated by a tight-binding square lattice with lattice constant a . The vector potential is included as the Peierls' phase factor [$\exp(-ie/\hbar \int_1 \vec{A} \cdot d\vec{l})$] in hopping matrix elements. While most previous studies have chosen the Landau gauge for this approach, the symmetric gauge is essential in our work, which modifies the approach [15].

The behavior of $T(\alpha)$ can be classified by γ (see Fig. 3). For $\gamma > 0$, $T(\alpha)$ is quantized when $l_{B^*} < r_0$. In this case, the magnetic confinements are similar to the harmonic potential. Thus, when edge channels pass the constriction

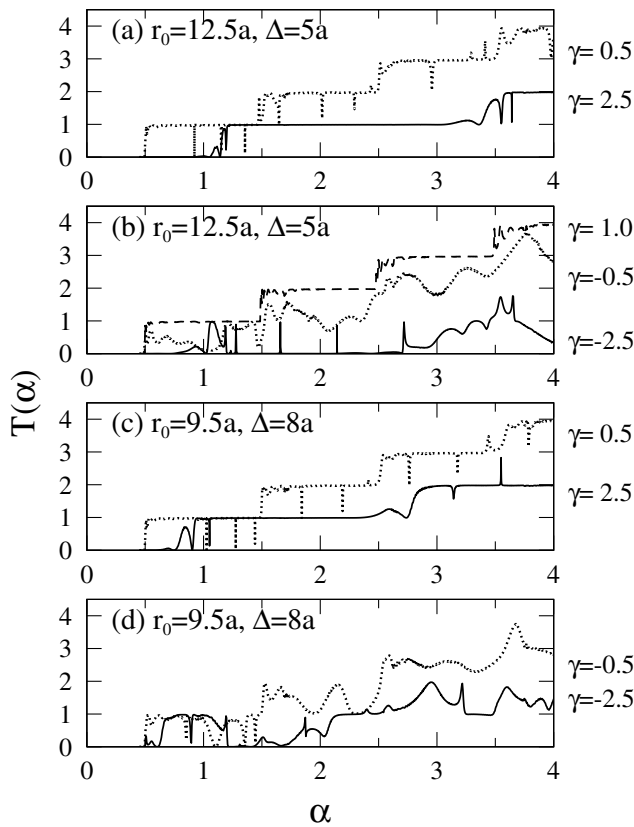


FIG. 3. $T(\alpha)$ for some γ 's and r_0 's. For all cases, $L_y = 35a$ and $l_{B_0}(0) = 5a$.

between the dot and wire edge, they are still well confined near the wire edge, without the interaction with those in the opposite edge, resulting in the quantization of $T(\alpha)$.

For $\gamma > 1$, $T(\alpha)$ is smaller than that of the uniform-field case with $\gamma = 1$, as in the case of electrostatic antidots [13]. This feature results from the fact that some incident edge channels are reflected by the dot due to the magnetic energy E^* larger than E_0 . As Δ decreases, the transition energy $E_t(j)$, where T changes from j to $j + 1$, increases from $E_0(j)$ to $E^*(j)$ and the number of resonances decreases [see Figs. 3(a) and 3(c)], because the magnetic edge states are confined in a narrower region. For $0 < \gamma < 1$, $T(\alpha)$ is the same as that for $\gamma = 1$ except for resonant dips. In this case, since $E^* < E_0$, the dot does not reflect any incident edge channels and binds electrons, as in the case of electrostatic dots; thus, the magnetic dot behaves as a resonator. More resonances occur as γ decreases from 1 and r_0 increases.

The features for $\gamma < 0$ are very different from those for $\gamma > 0$ and those by electrostatic modulations. For $-1 < \gamma < 0$, $T(\alpha)$ is not quantized and smaller than that of the uniform-field case, although $E^* < E_0$, in contrast to the case of $0 < \gamma < 1$. For $\gamma < -1$, $T(\alpha)$ is not quantized. Moreover, when $\Delta \approx l_{B_0}(0)$, all incident channels are completely reflected in some ranges of α , except for resonances, so that $G(\alpha)$ oscillates between 0 and G_0 with

the plateaus of $G = 0$, in marked contrast to the magnetic dot with $\gamma > 1$.

The features for $\gamma < 0$ result from the double-well and merged-well magnetic confinements, which are caused by the field reversal. To understand this behavior, we imitate the region near the dot by a magnetic step [6] in an infinite square well $U(y)$ with width L_y , which is divided into three strips by different magnetic fields; $B = B^*$ in the middle strip ($|y| < r_0$), while $B = B_0$ in the upper ($y > r_0$) and lower ones ($y < -r_0$). Its eigenstates can be written as $e^{ikx}Y_k(y)$, and $V_{\text{eff}}(y, k)$ is defined in a similar way to the dot case; $V_{\text{eff}}(y, k) = \hbar^2\{k + F(y)/l_{B_0}^2\}^2/(2m^*) + U(y)$, where $F(y)$ is $y + r_0(\gamma - 1)y/|y|$ for $|y| > r_0$ and γy for $|y| < r_0$. In Fig. 4, $V_{\text{eff}}(y)$'s and the calculated energy levels $E(k > 0)$'s are shown; note that $E(k < 0) = E(|k|)$. The states near $y = \pm L_y/2$ correspond to the current-carrying conventional edge states, while those near $y = \pm r_0$ to the magnetic edge states circulating around the dot. The triple wells [solid and dashed lines in Figs. 4(a) and 4(b)] correspond to the double-well magnetic confinements of the magnetic dot, while the double wells (dotted lines) to the merged-well ones.

For $-1 < \gamma < 0$, as $\Delta (= L_y/2 - r_0)$ decreases, the edge states with a given energy near $y = -L_y/2$ are determined by V_{eff} with smaller $k > 0$, which has a smaller barrier at $y = -r_0$, due to the wire confinement [see Fig. 4(a)]. When $\Delta \approx l_{B_0}$, the barrier is so small that the states near $y = -L_y/2$ can be easily extended to the middle or upper strip. The same behavior arises in the case of the magnetic dot. When $\Delta \approx l_{B_0}$, the conventional edge channels can interact with the double-well magnetic confinement with a small barrier, so that they are extended in the transverse direction. Then, the left-going channels easily interact with the right-going ones, thus,

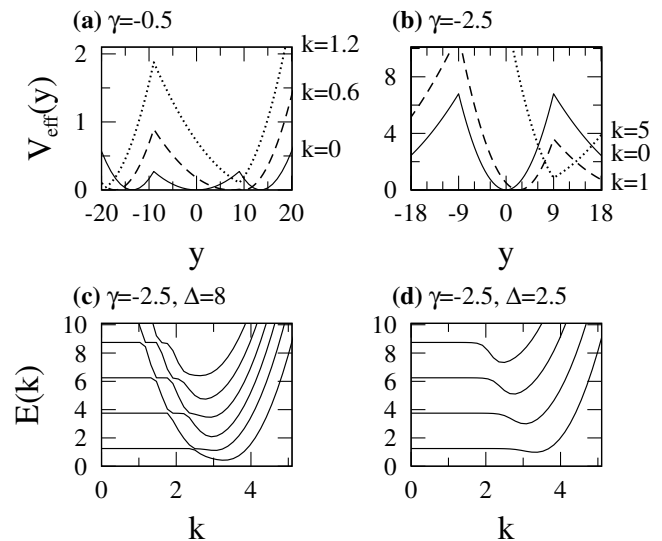


FIG. 4. (a),(b) $V_{\text{eff}}(y, k)$'s and (c),(d) $E(k)$'s for magnetic steps. The energy unit is $2E_0(0)$ while the length unit is arbitrary. For all cases, $l_{B_0}(0) = 2.47$ and $r_0 = 9$.

the conductance is not quantized, well corresponding to the classical trajectories in Fig. 1.

For $\gamma < -1$ and $k > 0$, when $l_{B_0} \ll \Delta < |\gamma|r_0$, the states confined in the local minimum at $y = L_y/2$ of the triple wells are the conventional edge states [see Fig. 4(b)]. Their energies are much higher than E_0 at $k = 0$ and satisfy $dE/dk < 0$. As Δ decreases, the well at $y = L_y/2$ becomes narrower, so that these states have higher energies and begin to be mixed with the magnetic edge states near $r = r_0$, resulting in level splitting. The number of the pure conventional edge channels near $y = L_y/2$ is $\sim M$, where M is the largest number satisfying $2l_{B_0}(M - 1) < \Delta$. In Fig. 4(c), the energy levels of two pure channels are shown; note that the levels of channels near $y = -L_y/2$ do not appear because of their very high energies. When $\Delta \approx l_{B_0}(0)$, there exist no pure conventional edge channels. In this case, eigenstates are classified into those with $dE/dk = 0$ inside the middle strip, those with $dE/dk > 0$ caused by the merged wells at $y = r_0$, and those with $dE/dk < 0$ which are the mixed ones of the magnetic and conventional edge states due to the triple wells with a small barrier at r_0 [see Fig. 4(d)]. Only the third ones propagate in the same direction as the conventional edge states, and they are not allowed in some energy ranges above E^* 's because of the state mixing. This feature indicates that all conventional edge channels can not pass the constriction between the magnetic dot and wire edge, i.e., $G(E_F) = 0$, in some ranges above E^* 's. The plateaus of $G(E_F) = 0$ appear in wider energy ranges for larger $|\gamma|$, smaller E_F , and smaller Δ . The resonant peaks in the ranges of $T(\alpha) = 0$ in Fig. 3(b) result from the snake magnetic edge states in the merged-well magnetic confinements.

Magnetic modulations with an order of ~ 1 T [$\alpha \sim 2$ for electron density of 10^{11} cm $^{-2}$ and $l_{B_0}(1) \sim 45$ nm] have been realized for both $\gamma > 0$ and $\gamma < 0$ in non-planar 2DEGs [3], while those of ~ 0.1 T [$\alpha \sim 20$ and $l_{B_0}(19) \sim 500$ nm] in magnetic steps [4]. When a magnetic dot or a finite step is formed by such modulations, our findings can be observed, because the magnetic confinements for $\gamma < 0$ ($\gamma > 0$) still form the double wells or merged wells (harmonic-like potentials). The modulations in Ref. [3] can be considered as a magnetic dot with very large r_0 and $\Delta = 0$. We propose that the constrictions between a magnetic dot and wire edges behave as a *magnetic quantum point contact*. The conductance in this new device with $\gamma > 1$ is similar to that in electrostatic contacts [16], while for $\gamma < -1$, it can be very different, showing a switching behavior with the plateaus of $G(E_F) = 0$.

In conclusion, we find that a magnetic quantum dot in a quantum wire behaves as a characteristic transmission barrier and a resonator. The double-well and merged-well

magnetic confinements caused by the field reversal at the dot boundary result in distinct magnetic edge states and transport properties, such as the nonquantized conductance and the plateaus of $G = 0$. The magnetic confinements are important to understanding the electronic and transport properties of other magnetic structures.

We are grateful to Professor F.M. Peeters for sending copies of his works. This work was supported by the QSRC at Dongguk University.

*Present address: Max-Planck-Institute for the Physics of Complex Systems, D-01187 Dresden, Germany.

- [1] M. A. McCord and D. D. Awschalom, *Appl. Phys. Lett.* **57**, 2153 (1990).
- [2] H. A. Carmona *et al.*, *Phys. Rev. Lett.* **74**, 3009 (1995); P. D. Ye *et al.*, *Phys. Rev. Lett.* **74**, 3013 (1995); A. Nogaret *et al.*, *Phys. Rev. B* **55**, R16037 (1999).
- [3] M. L. Leadbeater *et al.*, *J. Phys. Condens. Matter* **7**, L307 (1995); *Phys. Rev. B* **52**, R8629 (1995).
- [4] A. Nogaret, S. J. Bending, and M. Henini, *Phys. Rev. Lett.* **84**, 2231 (2000).
- [5] R. G. Mints, *JETP Lett.* **9**, 387 (1969); J. E. Müller, *Phys. Rev. Lett.* **68**, 385 (1992).
- [6] B.-Y. Gu *et al.*, *Phys. Rev. B* **56**, 13434 (1997); J. Reijniers and F. M. Peeters, *Phys. Rev. B* **63**, 165317 (2001).
- [7] A. Matulis, F. M. Peeters, and P. Vasilopoulos, *Phys. Rev. Lett.* **72**, 1518 (1994); J. Reijniers, F. M. Peeters, and A. Matulis, *Physica (Amsterdam)* **6E**, 759 (2000).
- [8] F. M. Peeters and P. Vasilopoulos, *Phys. Rev. B* **47**, 1466 (1994).
- [9] H.-S. Sim *et al.*, *Phys. Rev. Lett.* **80**, 1501 (1998).
- [10] J. Reijniers, F. M. Peeters, and A. Matulis, *Phys. Rev. B* **59**, 2817 (1999).
- [11] B. I. Halperin, *Phys. Rev. B* **25**, 2185 (1982); M. Büttiker, *Phys. Rev. B* **38**, 9375 (1988).
- [12] J. K. Jain and S. A. Kivelson, *Phys. Rev. Lett.* **60**, 1542 (1988).
- [13] Y. Takagaki and D. K. Ferry, *Phys. Rev. B* **48**, 8152 (1993).
- [14] Let us consider a state with $m' < 0$ [$\psi_{m'} = e^{im'\theta} R_{m'}(r)$] in the uniform field B_0 . This state is located at $r_p(m', B_0)$ and encloses $|m'|$ flux quanta. If s flux quanta are removed inside r_0 ($\ll r_p$), $\psi_{m'}$ can be written as $e^{i(m'+s)\theta} R_{m'}(r)$ due to the gauge invariance and then rewritten as $e^{im'\theta} R_{m_{\text{eff}}}(r)$.
- [15] To make $A = 0$ in leads [13], which are the wire regions of $|x| > L_x/2$, we choose that $B = 0$ for $r > r_1$ ($\gg r_0$) and $A = 0$ for $r > r_2$ ($\sim L_x/2$), where $r_1 = 38a$ and $L_x = 4000a$. This choice of A does not affect our results only when $L_y/L_x \ll 1$; otherwise, the Peierls' phase is counted incorrectly. To imitate the continuum limit, the condition $|2\pi Ba^2/\phi_0| \ll 1$ should be satisfied.
- [16] B. J. van Wees *et al.*, *Phys. Rev. Lett.* **60**, 848 (1988); D. A. Wharam *et al.*, *J. Phys. C* **21**, L209 (1988).